Published in IET Microwaves, Antennas & Propagation
Received on 30th May 2013
Revised on 31st August 2013
Accepted on 10th October 2013
doi: 10.1049/iet-map.2013.0287

ISSN 1751-8725

Electronically reconfigurable uni-planar antenna for cognitive radio applications

Gijo Augustin, Bybi P. Chacko, Tayeb A. Denidni

Department of Energy, National Institute of Scientific Research, Centre-Energy Materials and Telecommunication, National Institute of Scientific Research (INRS), University of Quebec, Montreal QC, Canada H5A 1K6
E-mail: augustin@emt.inrs.ca

Abstract: A single port, electronically reconfigurable, uni-planar antenna for cognitive-radio (CR) systems is presented. This design effectively merges the time-domain properties of tapered slot antennas with uni-planar nature of coplanar waveguide (CPW). Two tapered slot antennas were excited through a CPW, which is embedded with a PIN diode controlled band-pass filter. The prototype fabricated on Rogers® RO3006 high-frequency laminate with dielectric constant 6.5, loss tangent 0.002 and thickness 1.28 mm facilitates $S_{11} < -10$ dB bandwidth from 1.6 to 6.0 GHz in the wide-band mode and 3.39 to 3.80 GHz in the narrow-band mode. The measured radiation characteristics show that the design is suitable for CR applications, in which a wide-band antenna is used for spectrum sensing and a narrow-band antenna for transmission. In addition, the measured time-domain characteristics of the antenna including group delay, impulse response and fidelity factor are presented. These indicate that the proposed antenna can also be used for microwave imaging devices that are connected to the host through high-speed worldwide interoperability for microwave access terminals. Finally, to assist antenna engineers working on industrial design, the housing effect on the prototype was also studied experimentally in frequency and time domains.

1 Introduction

The recent advancements in the field of wireless communications compared with the developments in the beginning of past decade are enormous. In this new era, devices such as tablet computers and smart phones are being integrated with plenty of services such as worldwide interoperability for microwave access (WiMax) and wireless local area networks. This rapidly growing number of integrated services results in spectrum congestion, especially in highly populated scenarios [1]. One of the fundamental solution for this emerging challenge is the concept of a cognitive radio (CR) system that can change its transmitter parameters by detecting the environment in which it operates [2]. Being one of the most sensitive components in any wireless communication system, these challenges have opened an entirely new paradigm in the requirement and selection of antennas for CR applications [3]. This has attracted many researchers around the globe in industry and academia [4–14]. Recently, a number of non-planar [4, 7] and planar [5, 6, 8–16] antennas for CR applications have been reported in single-port [4–11, 13–15] and dual-port [5, 8, 9, 12, 16] configurations. In [12], a compact wide-band monopole integrated with a reconfigurable narrow-band antenna is presented. This antenna provides isolation better than 15 dB across two ports excited through microstrip lines on either side of a high-frequency laminate. Another design in [9], creatively integrates a disc monopole with two ports disposed at opposite sides of a substrate. This interesting design employs coplanar waveguide (CPW) and microstrip line to feed the wide-band and narrow-band configurations, respectively, with an inter-port isolation better than 10 dB. These dual-port antenna systems are highly desired when the search for previously used channels is done during the signal transmission on the next channel. However, this requires high degree of isolation in the order of 80–100 dB between the search and communication antennas [3].

The electronic re-configurability between the wide and narrow-band characteristics of an antenna is desirable in scenarios such as IEEE 802.11 wireless rural area networks, where the spectrum sensing takes place during the intra-frame and inter-frame quite periods, when the transceiver is switched off [3]. In this perspective, several novel antenna concepts have also been developed [14, 17–19]. In [19], a unique design of frequency reconfigurable antenna composed of a coplanar line that can be electronically connected to either wide-band or narrow-band pin and in-turn operates in the corresponding bands. A printed Yagi–Uda dipole antenna with metallic reflector in [14] facilitates electronic tuning of frequency, while maintaining high gain. Both the antennas [17, 18] are vivaldi-based single-port designs with excellent re-configurability. However, most of these designs [11, 12, 14, 15, 17–19] require the antenna structure to be printed on either side of a dielectric substrate, thus demanding more careful alignment in the fabrication process, which is a disadvantage for the antenna implementation. On the other hand, few designs provide a good time-domain performance in the wide-band mode [16–18], which is

add-on characteristics that enable the antenna to receive high-frequency impulses with less distortion. Previously, we have demonstrated a two-port CR antenna design in uni-planar configuration which effectively utilises the space between two wide-band tapered slot antennas for the integration of a narrow-band antenna, without disturbing the time-domain characteristics [16]. However, as pointed out in [3], our earlier design lacks high inter-port isolation in the order of 80–100 dB and similar radiation patterns when operates in wide-band and narrow-band modes. This results in the degradation of overall antenna performance in critical scenarios.

In this paper, we cover an important extension of our previous work by introducing a new single-port design that facilitates electronic switching between wide-/narrow-band modes, while maintaining the uni-planar configuration. This eliminates the requirement for high degree of inter-port isolation and facilitates identical radiation patterns when operates in wide-/narrow-band mode. Furthermore, an additional tapered slot on the antenna enhances the cross-polar level and therefore better performance. Compared with the recent single port, reconfigurable CR antenna designs [11, 15], the proposed work demonstrates advantages of uni-planar design along with pulse reproduction capabilities.

2 Antenna configuration

The basic structure of the proposed geometry is based on the two-port CR antenna design [16], shown in Fig. 1*a*. In the proposed design, there are two major modifications. Firstly, the narrow-band slot antenna in the previous design is eliminated and an elliptically curved slot with geometrical parameters *rx*, *ry*, *g1*, *ly* and *r*1 is embedded in place. It helps to reduce the back lobes of the tapered slot antennas and in-turn enhances the cross-polar level [20] of the

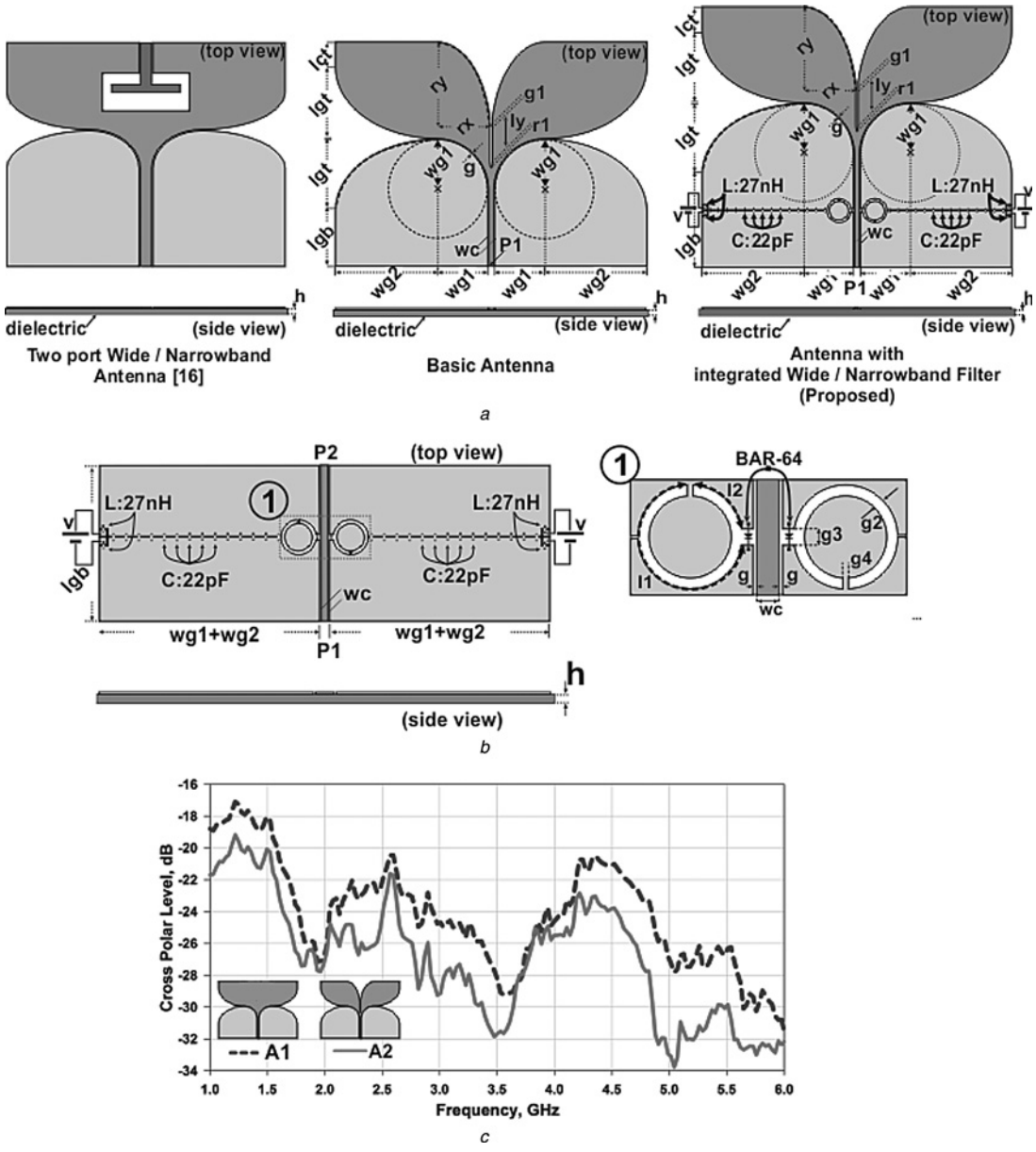

Fig. 1 *Evolution of the proposed antenna*

a Antenna geometry
b Wide-/narrow-band filter
c Measured cross-polar level

doi: 10.1049/iet-map.2013.0287

proposed antenna. This is evident from the measured cross-polar level displayed in Fig. 1*c*. Secondly, the electronic switching between the sensing and communication bands is achieved by employing a slot resonator-based filter inspired from [21] in the proposed antenna. The geometry of the filter is detailed in Fig. 1*b* with parameters *l*1, *l*2, *g*2, *g*3 and *g*4. It basically consists of two $\lambda g/4$ slot resonators with lengths *l*1 and *l*2 to generate two stop bands far spread out to form a pass band. To enable electronic control, Infineon® BAR-64 PIN diodes are embedded across the slot entrance from the CPW. On either side of the CPW ground plane, 0.2 mm width slots were created for DC isolation, which are loaded with 22 pF surface mount device (SMD) capacitors to maintain RF continuity. Finally, the bias lines were isolated from RF current using 27 nH chip inductors. The dimensions of the proposed design with design indications are outlined in Table 1. In the proposed work, computer simulation technology (CST) microwave studio is employed for design analysis and optimisation.

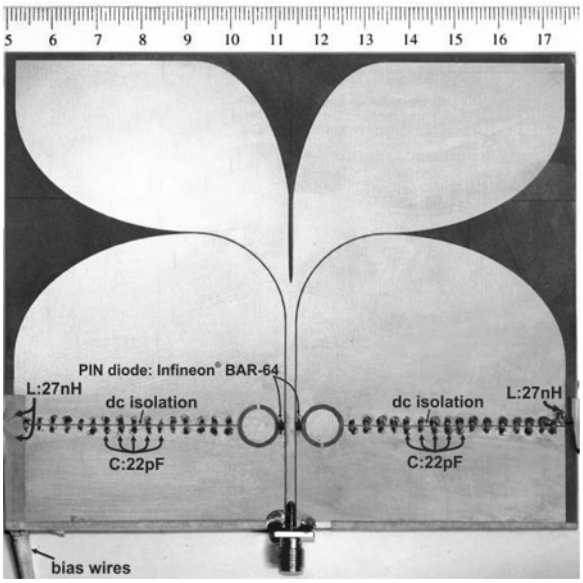

Fig. 2 *Photograph of the fabricated prototype*

3 Results and discussion

A prototype of the optimised antenna was fabricated on Rogers RO3006® high-frequency laminate with $\epsilon_r = 6.5$ and $h = 1.27$ mm. The photograph of the antenna is shown in Fig. 2. The measurements in frequency domain were carried out in an anechoic chamber using Agilent 8722ES vector network analyser. The time-domain measurements were carried out using Anritsu MS-4647A network analyser using two identical antenna prototypes.

3.1 Frequency domain

The simulated and measured reflection coefficients of the proposed antenna in wide-/narrow-band mode are plotted in Fig. 3. In the full wave simulator, PIN diodes were modelled using their equivalent circuit from the datasheet [23], as shown in the inset. The measured $S_{11} \leq -10$ dB bandwidths of the proposed antenna are from 1.6 to 6 GHz (PIN diode is ON) and from 3.39 to 3.80 GHz (PIN diode is OFF) when operating in wide-band and narrow-band modes, respectively. The discrepancies between the simulated and measured results are because of the approximations in the PIN diode model. The PIN diodes were represented in CST environment as lumped resistance, inductance, capacitance, which does not consider the influence of DC bias components. Although there are some offsets in frequency between the simulated and measured values, the trends are well predicted by the simulators.

A more detailed view about the operation of the antenna is obtained by analysing the narrow-band-pass filter separately. As detailed in Fig. 1*b*, the basic structure of the filter consists of two unequal ring resonators with lengths *l*1 and *l*2 across the CPW. The simulated S-parameters of the two-port narrow-band-pass filter are shown in Fig. 4, which clearly demonstrates two stop bands resonating at 2.42 GHz and 6.31 GHz along with a pass band at 3.54 GHz. A better understanding about the operation of the slot resonators was obtained through the surface current analysis. It can be clearly seen from Fig. 5*a* that the longer and shorter slot resonators are resonating at 2.45 and 6.31 GHz, respectively. As

Table 1 Detailed parameters of the proposed antenna

Parameters	Descriptions	Dimension, mm	Design indications
wc	centre conductor width of CPW	2	design a 50 Ω CPW line on a substrate with parameters *wg*1, *wc*, *g*, *lgb*, *h* and ϵ_r [22]
g	gap b/w ground and signal line of CPW	0.35	
lgb	length of CPW ground, first portion	37	
h	thickness of the laminate	1.27	
*wg*1	width of CPW ground	20	
ϵ_r	dielectric permittivity of the laminate	6.5	
lgt	*y*-radius of elliptical taper	28	the design parameters *lgt* and *wg*2 define the curvature length of the elliptical tapering. The lower cutoff frequency of the UWB antenna is determined by these two parameters [16]
*wg*2	*x*-radius of elliptical taper	40	
*g*2	width of the slot resonator	1	design two $\lambda g/4$ slot resonators with parameters *l*1, *l*2, *g*2, *g*3 and *g*4 to generate two stop bands far spread out to form a pass band [21]
*g*3	opening gap from CPW to slot resonator	1.5	
*g*4	gap between two slot resonators	2	
*l*1	length of slot resonator-1	20.64	
*l*2	length of slot resonator-2	5.71	
rx	*y*-radius of elliptical separation taper	21.35	the dimensions *rx*, *ry*, *ly*, *r*1, *lct* and *g*1 of elliptical separation taper are optimised through simulation for better cross-polar level with negligible influence on UWB and NB antenna performances
ry	*x*-radius of elliptical separation taper	38	
ly	length of the separation slot	20	
*r*1	*y*-radius of separation taper ending	3	
lct	extended length of centre taper	10	
*g*1	gap of separation tapering	1	

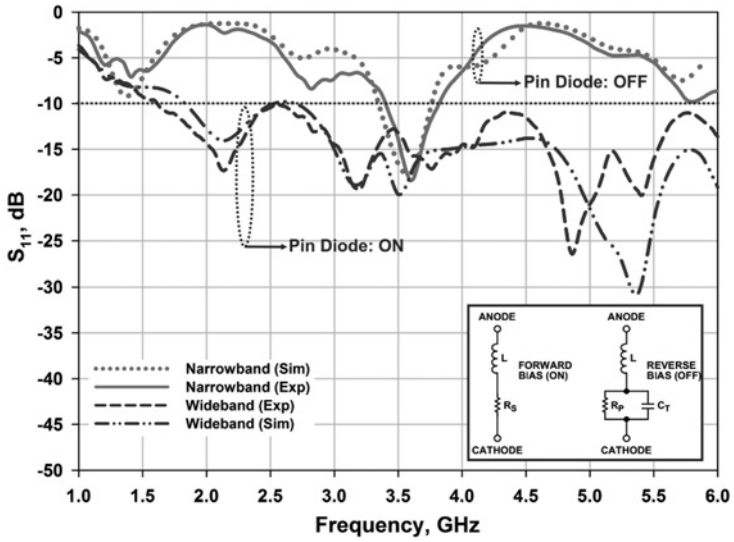

Fig. 3 *Measured and simulated S_{11} of the proposed antenna*

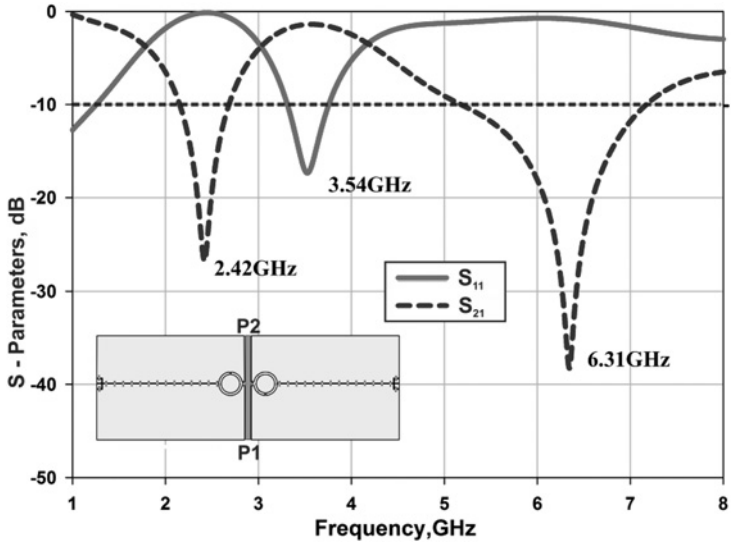

Fig. 4 *S-parameters of the narrow-band-pass filter*

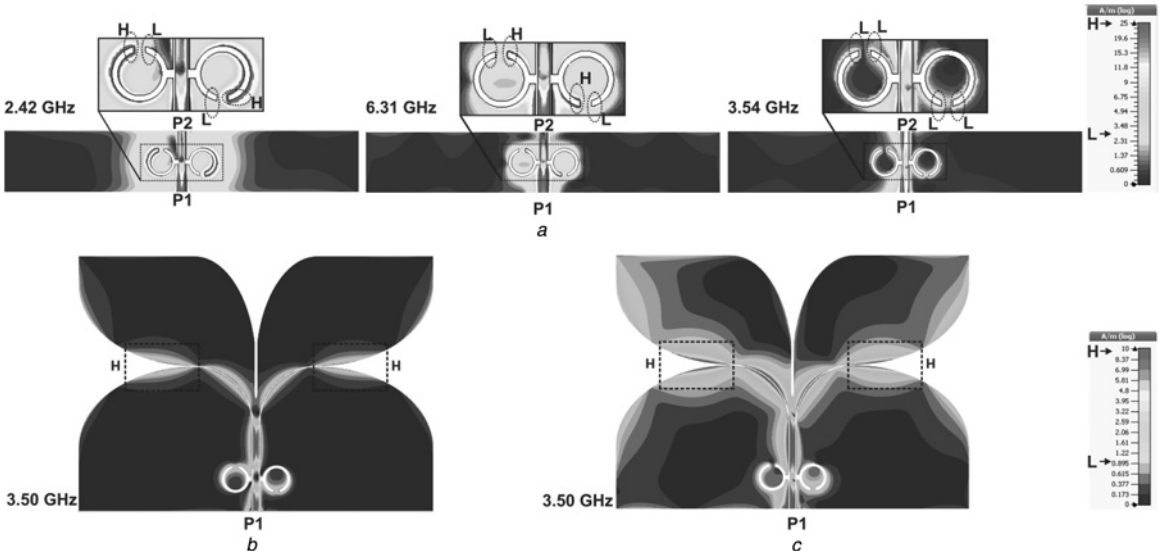

Fig. 5 *Simulated surface current distributions*

a Filter
b Integrated antenna in wide-band mode
c Integrated antenna in narrow-band mode

doi: 10.1049/iet-map.2013.0287

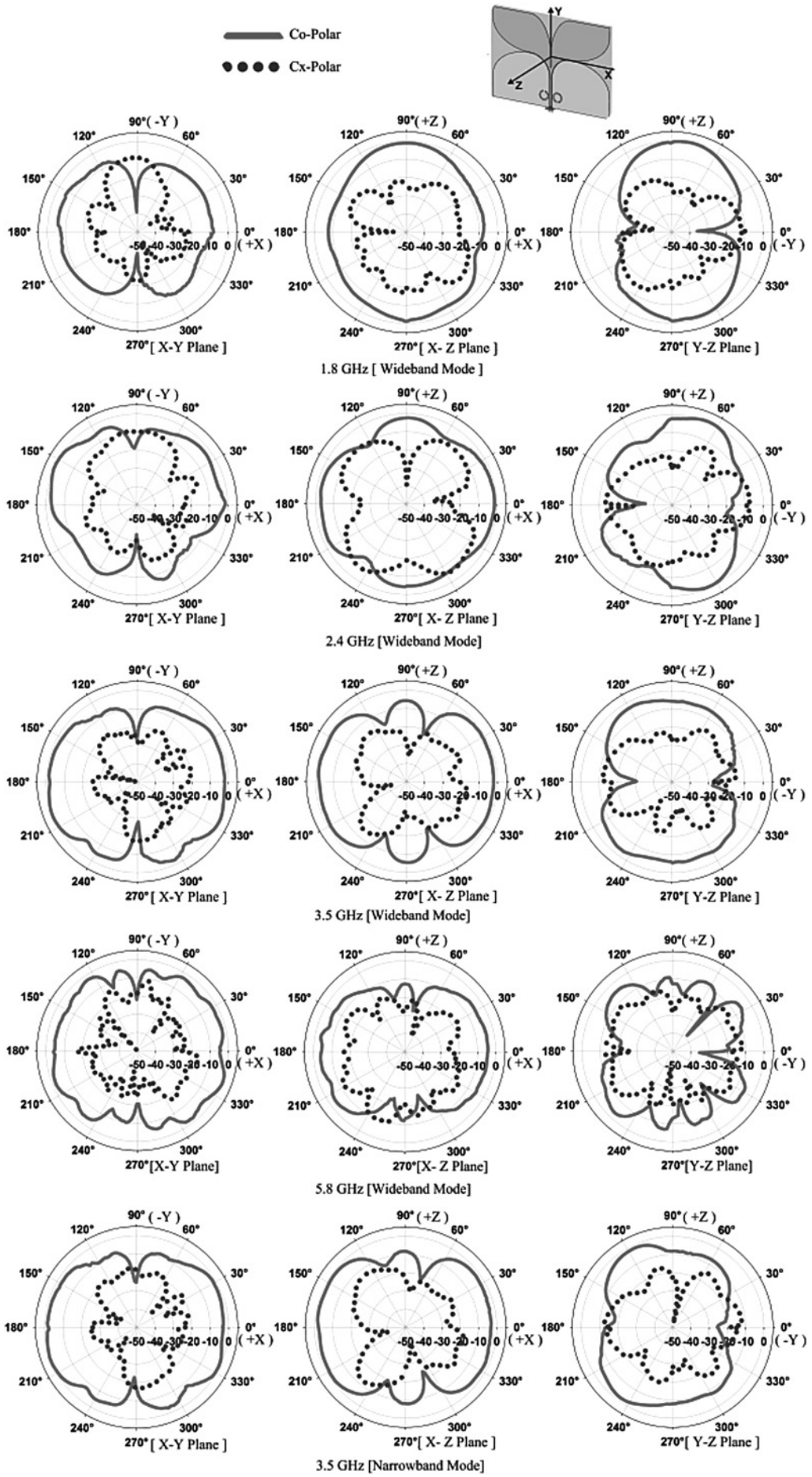

Fig. 6 *Measured radiation pattern of the antenna*

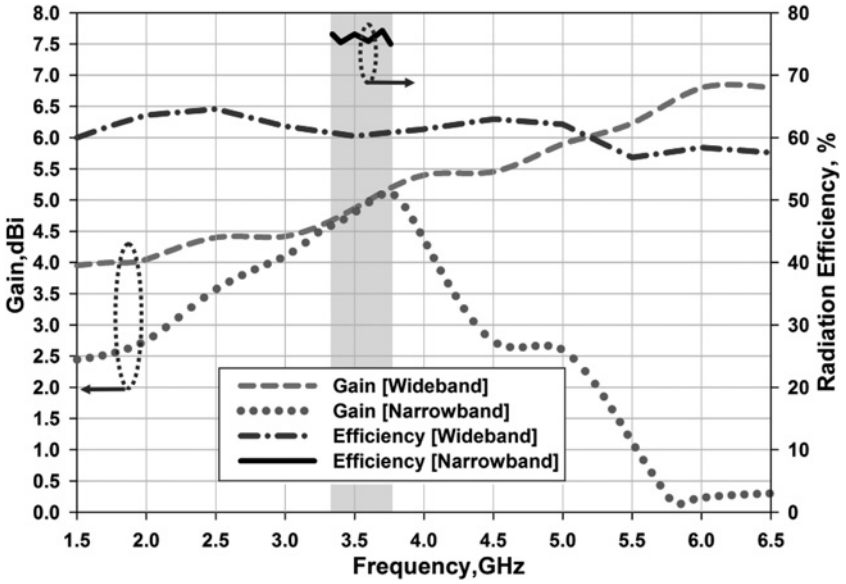

Fig. 7 *Separately measured gain and efficiencies of the antenna in wide-band mode (PIN: ON) and narrow-band mode (PIN: OFF)*

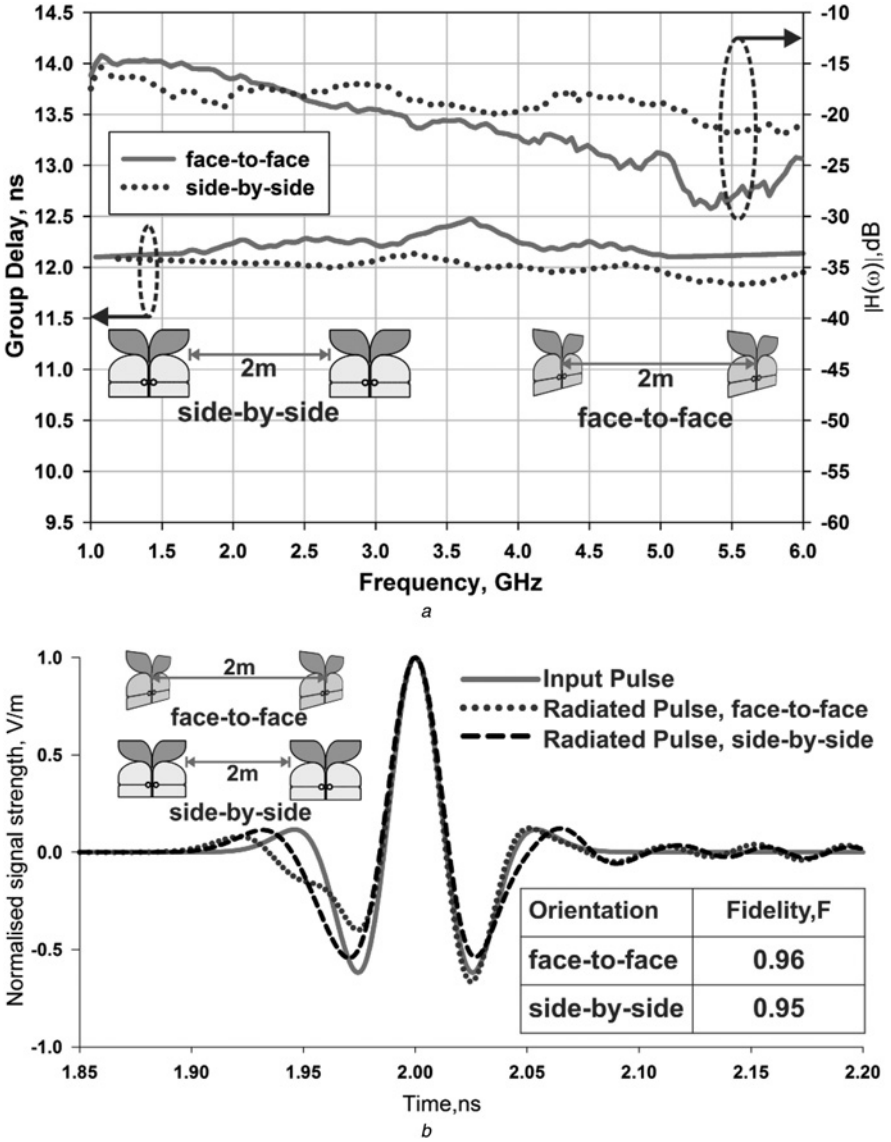

Fig. 8 *Measured time-domain characteristics of the antenna in wide-band mode*

a Group delay and normalised antenna transfer function in two different orientations
b Input and radiated pulses

doi: 10.1049/iet-map.2013.0287

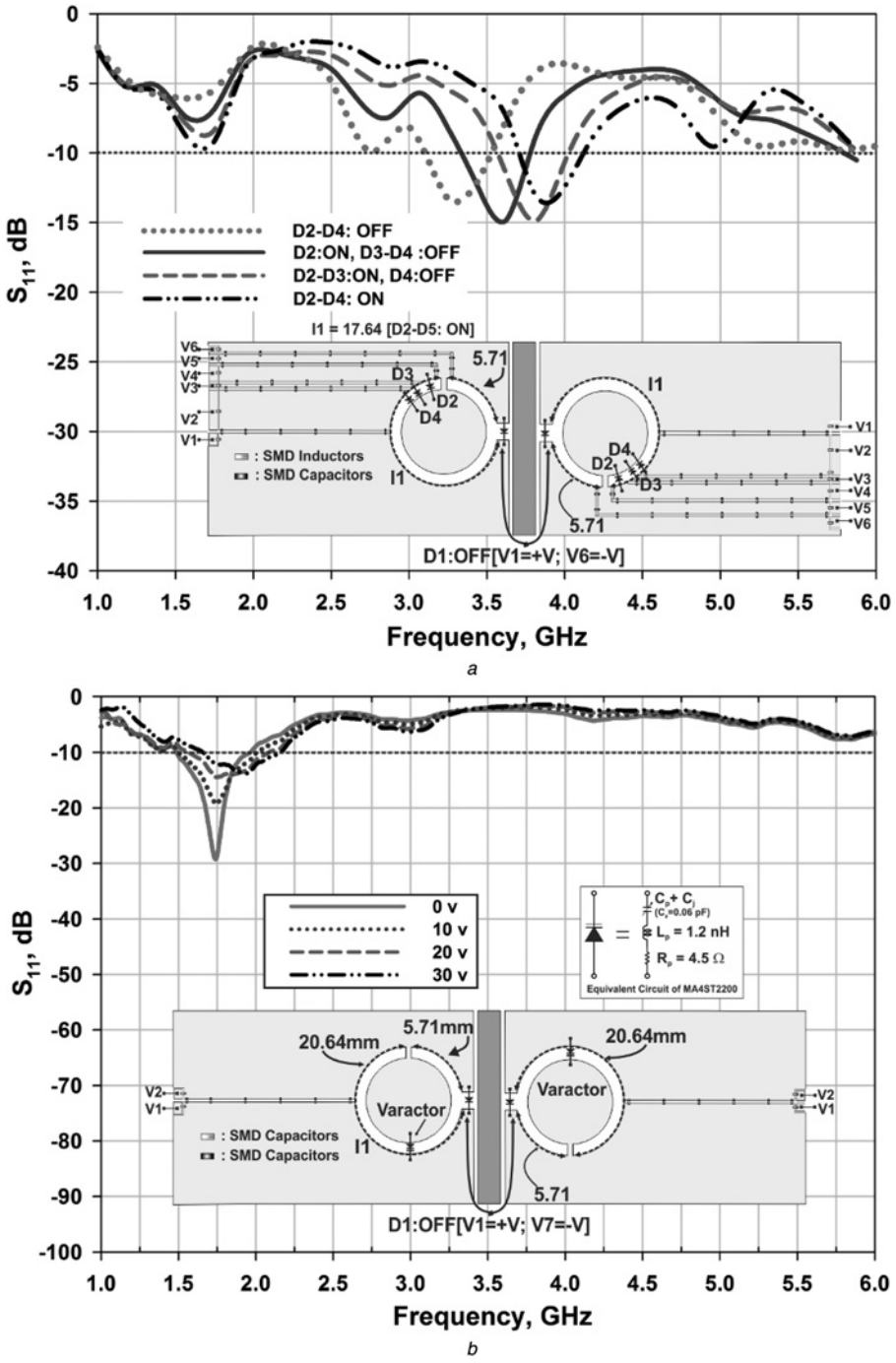

Fig. 9 *Measured narrow-band tuning of the proposed antenna*

a By reducing the length L1 using PIN diodes
b By changing the slot capacitance using varactor diodes

expected, at 3.54 GHz, when the filter operates in the pass-band, the current excitations on both the slot resonators are minimal.

The surface current on the proposed antenna, when operating in the wide-band mode and narrow-band mode at 3.5 GHz is also incorporated in Figs. 5*b* and *c*, respectively. It is clear that the tapered surface regions on both sides of the antenna, when operated in wide-/narrow-band modes, have high current excitations and thereby contribute to radiation. The radiation patterns of the proposed antenna in wide-band mode (PIN diode ON) and narrow-band mode (PIN diode OFF) are measured in *XZ*, *XY* and *YZ* planes and plotted in Fig. 6. The patterns are slightly directional throughout the band with good polarisation purity. It is also worth to note that the radiation pattern in the sensing (wide-band mode) and transmission mode (narrow-band mode) remains unaltered which is one of the key requirement for the CRs when operating in critical communication scenarios [3]. In general, the patterns are similar to those observed for antennas used in CR systems [15, 17, 19] and in high-speed WiMAX terminals [24].

The gains of the broad-band and narrow-band antenna configurations are independently measured using the gain comparison method [25] and are displayed in Fig. 7. In the wide-band mode, the gain found to be increased with frequency with variations upto 3 dBi. This trend is similar to those of Vivaldi antennas in which the radiating aperture is added with frequency. The effect of band rejection is clearly observed in the gain variations of narrow-band

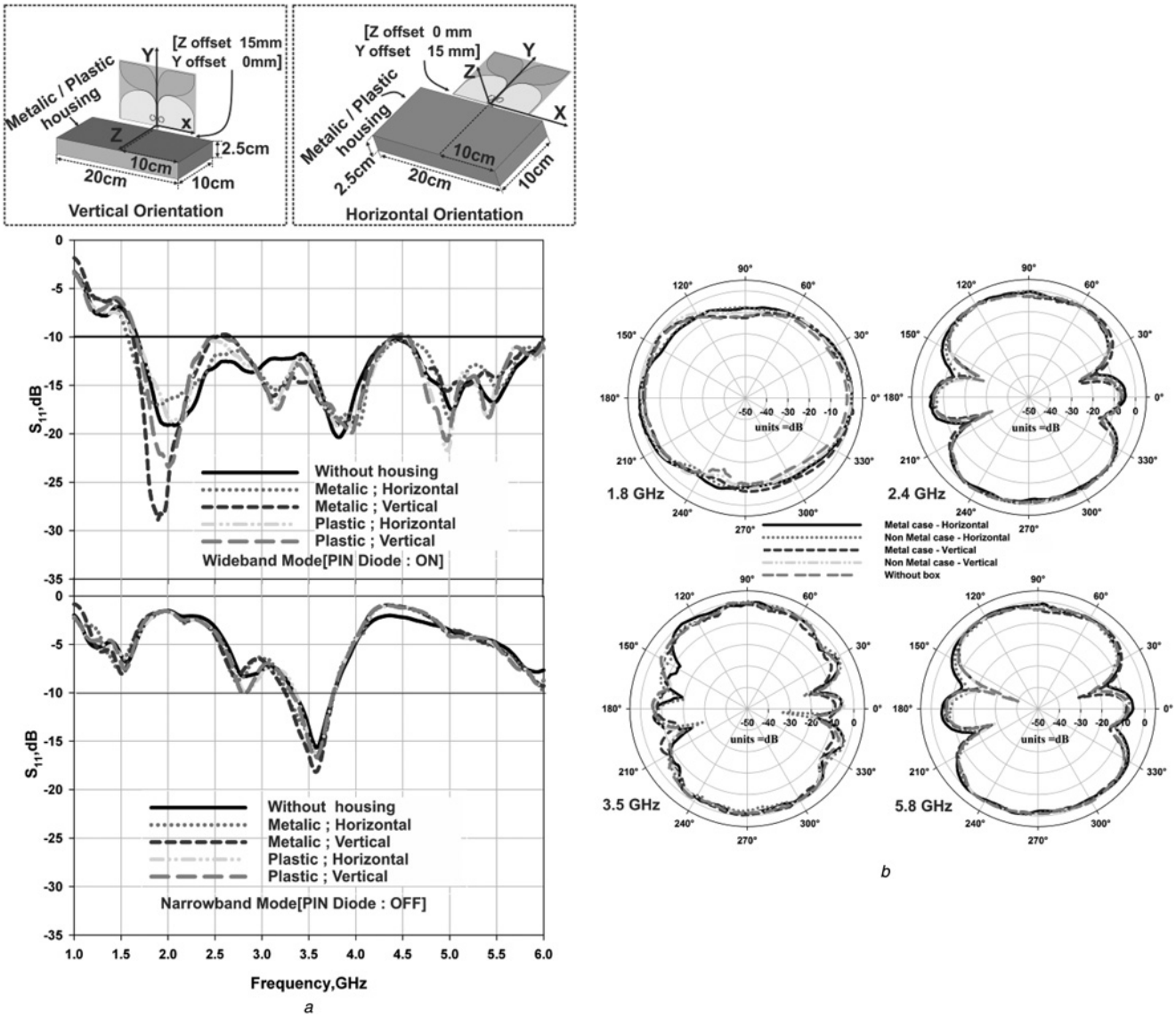

Fig. 10 *Measured housing effect in frequency domain*

a Reflection coefficient
b Radiation pattern in *XZ*-plane

antenna. This indicates that the antenna when operates in the NB mode is filtering the unwanted frequencies. The radiation efficiency of both the switching configurations were also measured independently using the wheeler cap method [26] and are incorporated in Fig. 7. The radiation efficiency is found to be better than 72% in the narrow-band configuration. In the wide-band mode (when PIN diode is ON), the efficiency is found to be better than 58%. The difference in antenna efficiency is because of the series resistance of the PIN diodes that yield to thermal loses [27, 28].

3.2 Time domain

The time-domain characteristics of the proposed antenna when operated in wide-band mode are also measured and analysed. The group delay, antenna transfer function, impulse response and fidelity factor help to evaluate the influence of the antenna on high-frequency impulses when transmitted or received. Fig. 8*a* shows the measured group delay of the proposed antenna using two identical prototypes in side-by-side and face-to-face orientation. The measurements were performed in an anechoic chamber using Anritsu MS-4647A vector network analyser. It is found that the group delay variations remain stable within 1 ns in both orientations. The transfer function of the antenna is also evaluated using (1)

$$H(\omega) = \sqrt{\frac{2\pi RcS_{21}(\omega)e^{j\omega R/c}}{j\omega}} \tag{1}$$

where c is the velocity of light and R is the distance between the identical antennas [29].

It is clear from Fig. 8*a* that the antenna transfer function remains fairly flat with variations <15 dB throughout the band in both orientations. The impulse response of the antenna is studied by convoluting the fourth derivative of Gaussian pulse (2), with $h(t)$, inverse Fourier transform of (1).

$$V_{in}(t) = A\left[3 - 6(4\pi/T^2)t^2 + (4\pi/T^2)t^4\right] \exp\left(-2\pi(t/T)^2\right) V/m \tag{2}$$

The spectrum of this impulse covers the Federal Communication Commission emission mask when the

doi: 10.1049/iet-map.2013.0287

amplitude constant, 'A' is 1.6 and pulse duration, 'T' is 67 ps. The impulse response shown in Fig. 8*b* reveals that the antenna retains the pulse shape both in the face-to-face and side-by-side orientations without much dispersion.

The fidelity factor (3) [30] provides a quantitative measure of pulse distortion which is calculated from the input and radiated pulses at different orientations and is incorporated in the inset table of Fig. 8*b*

$$F = \frac{\int_{-\infty}^{\infty} S_t(t) S_r(t-\tau) d_t}{\sqrt{\int_{-\infty}^{\infty} |S_t(t)|\, \mathrm{d}t \int_{-\infty}^{\infty} |S_t(t-\tau)| d_t}} \quad (3)$$

It is found that $F > 0.94$ in both orientations clarifying that the antenna is capable of handling the high-frequency impulses.

3.3 Narrow-band tuning

The unique CPW-based design of the slot resonator-based filter facilitates electronic tuning of the operating frequency, when operates in the narrow-band mode. Two interesting designs that facilitate narrow-band tuning are experimentally demonstrated in Fig. 9. First, by activating three RF PIN diode switches placed across the slot and thereby varying the effective length of the larger resonator ($l1$). As shown in the inset of Fig. 9*a*, the bias network for this electronic tuning consists of very thin DC isolation lines of width 0.2 mm. The RF continuity across these lines are ensured by integrating 22 pF SMD capacitors across the slots in every 8 mm. The bias lines $V1$–$V6$ are isolated from the RF signal using 27 nH chip inductors.

The frequency tuning is illustrated in Fig. 9*a* by electronically reducing the effective length $l1$ from 20.64 to 17.64, which results a frequency shift from 3.3 to 3.9 GHz. Even though, the length of the shorter resonator remains constant, its resonant frequency varies slightly [21]. Thus the corresponding transmission zeros will be shifted and thereby the pass band in between them.

In another design, the narrow-band resonance is changed by varying the effective slot capacitance of the ring resonator. The longer slot of the resonator is loaded with a varactor diode, Skyworks-SMV1801 as shown at the inset of Fig. 9*b*. The orientation of PIN diode, $D1$ and the varactor diode are in such a way that the reverse bias condition for diode $D1$ switch the antenna into the narrow-band mode. By increasing this reverse bias voltage, diode $D1$ remains switched OFF; meanwhile the varactor diode changes its capacitance and in-turn varies the resonance frequency. It is found that by varying the bias

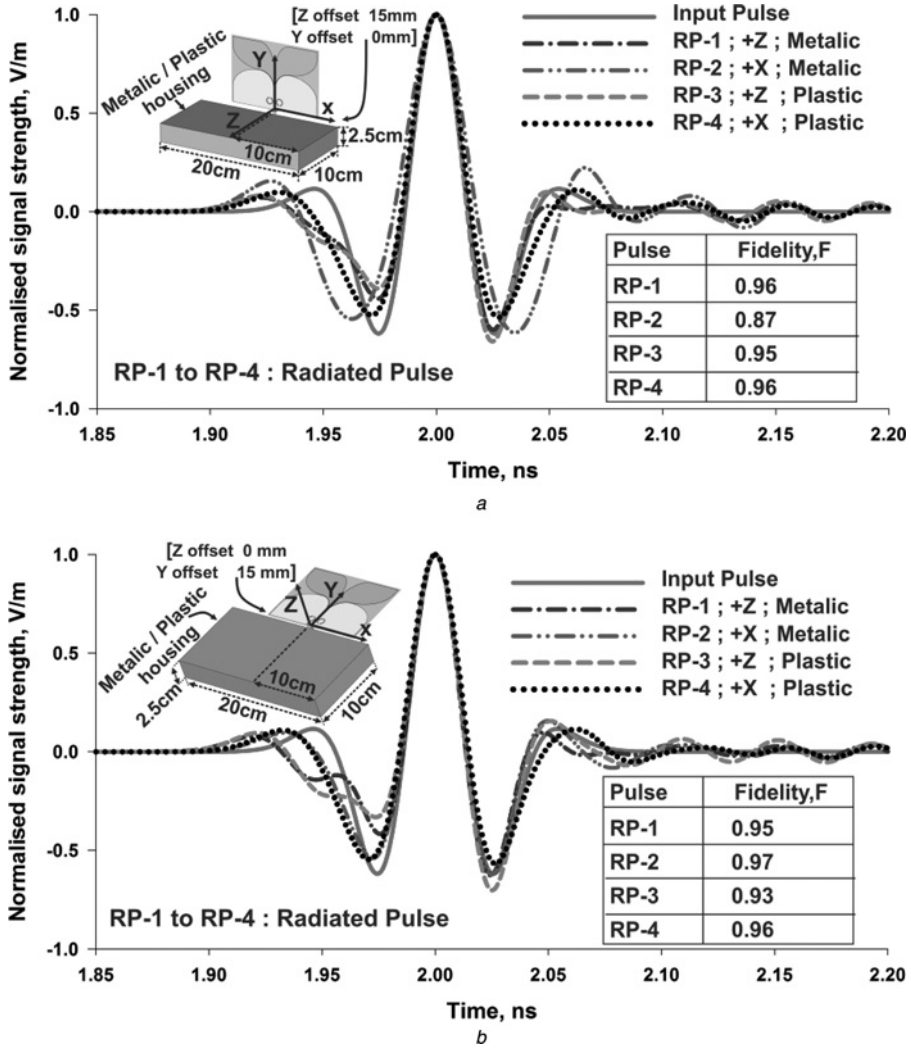

Fig. 11 *Measured pulse distortion analysis of the proposed antenna in the vicinity of plastic/metallic system housing*

a Vertical orientation
b Horizontal orientation

voltage from 0 to 30 v, the resonant frequency of the antenna is tuned from 1.74 to 1.94 GHz.

4 Housing effect

Since, mutual coupling from neighbouring objects influences the overall performance of printed antennas, it is desirable to study the housing effects on the antenna characteristics [30]. The experimental analysis was performed at different orientations in an anechoic chamber using metallic and plastic cases with dimension $20 \times 10 \times 2.5$ cm^3. It is found from frequency and time-domain measurements that the influence on the system housing is minimal, when the antenna is oriented 15 mm away from the casing. The reflection coefficient and radiation pattern in wide-/narrow-band mode at different orientations in the optimum mounting position are displayed in Figs. 10*a* and *b*, respectively. It is found that the variations are minimal when the antenna is mounted at the suggested offset from the housing. The pulse distortion analysis in the wide-band mode at the optimum housing position was also conducted. It is found from Fig. 11 that the impact on the radiated impulses in varied orientations is negligible. The fidelity factor remains >0.85, which clearly demonstrates that the antenna can effectively handle the high-frequency impulses when it is mounted on a metallic/plastic system housing.

5 Conclusion

An electronically switchable, single-port wide-/narrow-band antenna in uni-planar configuration for CR applications has been presented. The basic design of the antenna utilises two tapered slot antennas fed by a CPW-based electronically reconfigurable filter. The performances of the antenna in frequency and time domain have been analysed. The measurement results have shown that the antenna provides 2:1 voltage standing wave ratio bandwidth from 1.6 to 6 GHz and 3.39 to 3.80 GHz in wide- and narrow-band configurations, respectively. The radiation patterns in the sensing and transmission modes are found to be identical which is essential for crucial communication scenarios. In addition, a good time-domain response of the antenna indicates that the design is capable of distortion less transmission and reception of high-frequency impulses when operates in wide-band mode. Two design considerations for the electronic tuning of the antenna in narrow-band mode have also been experimentally demonstrated in this paper. Moreover, the experimental analysis in frequency and time domains has indicated that the proposed design is less disposed to the housing effects when mounted in metallic/plastic system casing. Therefore the proposed antenna can be a potential candidate for future CR systems, which may also analyse high-frequency impulses when operating in the wide-band mode.

6 References

1 Webb, W.: 'UK approach to regulating cognitive radio devices'. IET Cognitive Radio and Software Defined Radio: Technologies and Techniques Seminar, 2008

2 Federal Communications Commission: 'Spectrum policy task force', Report ET Docket, November 2002, (02–135)

3 Hall, P.S., Gardner, P., Faraone, A.: 'Antenna requirements for software defined and cognitive radios', *Proc. IEEE*, 2012, **100**, (7), pp. 2262–2270

4 Wang, Z.P., Hall, P.S., Kelly, J., Gardner, P.: 'Tem horn circular array for wide band pattern notch reconfigurable antenna system', Proc. Antennas and Propagation Conf. (LAPC), Loughborough, UK, November 2010, pp. 365–367

5 Ebrahimi, E., Hall, P.S.: 'A dual port wide-narrowband antenna for cognitive radio'. Proc. Third European Conf. Antennas and Propagation, EuCAP 2009, Berlin, Germany, March 2009, pp. 809–811

6 Tawk, Y., Costantine, J., Avery, K., Christodoulou, C.G.: 'Implementation of a cognitive radio front-end using rotatable controlled reconfigurable antennas', *IEEE Trans. Antennas Propag.*, 2011, **59**, (5), pp. 1773–1778

7 Wu, T., Rong Lin, L., Soon Young, E., *et al.*: 'Switchable quad-band antennas for cognitive radio base station applications', *IEEE Trans. Antennas Propag.*, 2010, **58**, (5), pp. 1468–1476

8 Kelly, J.R., Ebrahimi, E., Hall, P.S., Gardner, P., Ghanem, F.: 'Combined wideband and narrowband antennas for cognitive radio applications'. Proc. IET Seminar on Cognitive Radio and Software Defined Radios: Technologies and Techniques, September 2008, pp. 1–4

9 Ghanem, F., Hall, P.S., Kelly, J.R.: 'Two port frequency reconfigurable antenna for cognitive radios', *Electron. Lett.*, 2009, **45**, (11), pp. 534–536

10 Jin, G.P., Zhang, D.L., Li, R.L.: 'Optically controlled reconfigurable antenna for cognitive radio applications', *Electron. Lett.*, 2011, **47**, (17), pp. 948–950

11 Aboufoul, T., Alomainy, A., Parini, C.: 'Reconfiguring Uwb monopole antenna for cognitive radio applications using gaas fet switches', *IEEE Antennas Wirel. Propag. Lett.*, 2012, **11**, pp. 392–394

12 Erfani, E., Nourinia, J., Ghobadi, C., Niroo-Jazi, M., Denidni, T.A.: 'Design and Implementation of an Integrated Uwb/reconfigurable-slot antenna for cognitive radio applications', *IEEE Antennas Wirel. Propag. Lett.*, 2012, **11**, pp. 77–80

13 Tawk, Y., Christodoulou, C.G.: 'A new reconfigurable antenna design for cognitive radio', *IEEE Antennas Wirel. Propag. Lett.*, 2009, **8**, pp. 1378–1381

14 Cai, Y., Guo, Y.J., Bird, T.S.: 'A frequency reconfigurable printed Yagi-Uda dipole antenna for cognitive radio applications', *IEEE Trans. Antennas Propag.*, 2012, **60**, (6), pp. 2905–2912

15 Boudaghi, H., Azarmanesh, M., Mehranpour, M.: 'A frequency-reconfigurable monopole antenna using switchable slotted ground structure', *IEEE Antennas Wirel. Propag. Lett.*, 2012, **11**, pp. 655–658

16 Augustin, G., Denidni, T.A.: 'An integrated ultra wideband/narrow band antenna in uniplanar configuration for cognitive radio systems', *IEEE Trans. Antennas Propag.*, 2012, **60**, (11), pp. 5479–5484

17 Hamid, M.R., Gardner, P., Hall, P.S., Ghanem, F.: 'Switched-band vivaldi antenna', *IEEE Trans. Antennas Propag.*, 2011, **59**, (5), pp. 1472–1480

18 Hamid, M.R., Gardner, P., Hall, P.S., Ghanem, F.: 'Vivaldi antenna with integrated switchable band pass resonator', *IEEE Trans. Antennas Propag.*, 2011, **59**, (11), pp. 4008–4015

19 Ghanem, F., Ghanem, K., Hall, P.S., Hamid, M.R.: 'A miniature frequency reconfigurable antenna for cognitive radios'. Proc. IEEE Int. Symp. Antennas and Propagation (APSURSI 2011), Washington, USA, July 2011, pp. 171–174

20 Gazit, E.: 'Improved Design of the Vivaldi Antenna', *IEE Proc. H Microw. Antennas Propag.*, 1998, **135**, (2), pp. 89–92

21 El-Shaarawy, H.B., Coccetti, F., Plana, R., El-Said, M., Hashish, E.A.: 'Novel reconfigurable defected ground structure resonator on coplanar waveguide', *IEEE Trans. Antennas Propag.*, 2010, **58**, (11), pp. 3622–3628

22 Simons, R.N.: 'Coplanar waveguide circuits and components and systems' (Wiley-Interscience, Hoboken, 2001), pp. 20–21

23 'Datasheet Bar 64 Series', Available at http://www.infineon.com

24 Wong, K.L.: 'Planar antennas for wireless communication', (John Wiley & Songs, Inc., New Jersey, 2003)

25 Balanis, C.A.: 'Antenna theory: analysis and design', (John Wiley & Songs, Inc., New Jersey, 1997)

26 Huang, Y., Lu, Y., Boyes, S., Chattha, H.T., Khiabani, N.: 'Wideband antenna efficiency measurements'. Proc. Int. Workshop on Antenna Technology (iWAT-2010), March 2010, pp. 1–4

27 Artiga, X., Perruisseau-Carrier, J., Pardo-Carrera, P., Llamas-Garro, I., Brito-Brito, Z.: 'Halved vivaldi antenna with reconfigurable band rejection', *IEEE Antennas Wirel. Propag. Lett.*, 2011, **10**, pp. 56–58

28 Perruisseau-Carrier, J., Pardo-Carrera, P., Miskovsky, P.: 'Modeling, design and characterization of a very wideband slot antenna with reconfigurable band rejection', *IEEE Trans. Antennas Propag.*, 2010, **58**, (7), pp. 2218–2226

29 Sörgel, W., Wiesbeck, W.: 'Influence of the antennas on the ultra-wideband transmission', *Eurasip J. Appl. Signal Process.*, 2005, **2005**, pp. 296–305

30 Telzhensky, N., Leviatan, Y.: 'Novel method of Uwb antenna optimization for specified input signal forms by means of genetic algorithm', *IEEE Trans. Antennas Propag.*, 2006, **54**, (8), pp. 2216–2225

doi: 10.1049/iet-map.2013.0287